Dalton Transactions

This article can be cited before page numbers have been issued, to do this please use: S. Senthilkumar, M. S. Maru, R. S. Somani, H. C. Bajaj and S. Neogi, *Dalton Trans.*, 2017, DOI: 10.1039/C7DT03754F.

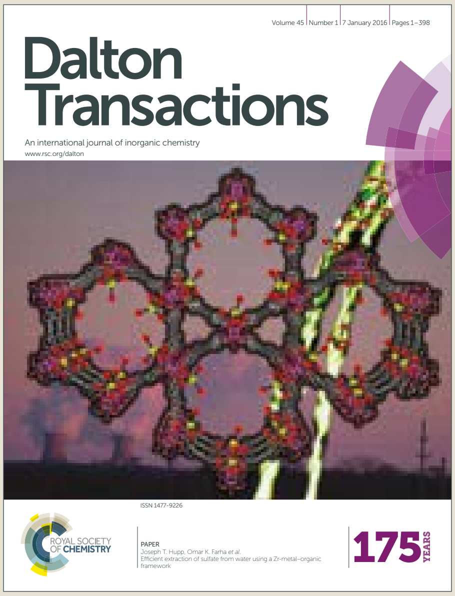

View Article Online
DOI: 10.1039/C7DT03754F

Journal Name

ARTICLE

Unprecedented NH_2–MIL–101(Al)/*n*–Bu_4NBr system as solvent free heterogeneous catalyst for efficient synthesis of cyclic carbonate via CO_2 cycloaddition

Received 00th January 20xx,
Accepted 00th January 20xx

DOI: 10.1039/x0xx00000x

www.rsc.org/

S. Senthilkumar, Minaxi S. Maru, R. S. Somani, H. C. Bajaj and Subhadip Neogi*

The amine functionalised framework NH_2-MIL-101(Al) is synthesized by solvothermal as well as microwave method and characterized by PXRD, FT-IR, TGA, SEM-EDX and BET surface area analysis. The desolvated framework, in the presence of co-catalyst tetra butyl ammonium bromide (TBAB), acts as excellent heterogeneous catalyst for the solvent free cycloaddition of carbon dioxide (CO_2) with epoxides, affording five-membered cyclic carbonates. Using styrene oxide, the NH_2-MIL-101(Al)/TBAB system shows more than 99% conversion with 96% yield, 99% selectivity, having turn over frequency (TOF) of 23.5 h^{-1}, and validates synergistic effect of quaternary ammonium salt during CO_2 cycloaddition. The catalyst could be recycled at least five times without noticeable loss of activity, while leaching test shows no leached Al^{3+} ion throughout the reaction. Thorough analysis of reaction parameters revealed optimum conditions for obtaining maximal yield with highest selectivity are: 6 h duration, 120 °C temperature, and 18 bar of CO_2 pressures. The outstanding conversion and selectivity is maintained for a range of aliphatic and aromatic epoxides, corroborating the duel benefit of micro-mesoporous system with amine functionality that offers easy accessibility of reactant molecules with diverse sizes, and provides an inspiration to future catalytic system for CO_2 cycloaddition. We also propose a rationalized mechanism for the cycloaddition reaction, mediated by NH_2-MIL-101(Al) and TBAB, on the basis of literature and experimental outcome.

Introduction

The rising level of carbon dioxide (CO_2)[1] in atmosphere is a major threat to global warming that has initiated several attempts for CO_2 capture processes. The more abundance of non-toxic and non-flammable CO_2 has inspired the scientific community to invent technologies of using CO_2 as C_1 feed stock for multipurpose synthesis. In this regard, the cycloaddition reaction of CO_2 with epoxide is a 100% atom economic reaction, constituting one of the most efficient ways of artificial CO_2 fixation. This chemistry is greener compared to the traditional synthesis, involving highly toxic and corrosive phosgene or isocyanates.[2] Furthermore, cyclic carbonate is of great industrial interest[3] because it finds worthy application[4] as green solvents,[5] electrolytes in lithium ion batteries[6] or in the pharmaceutical and fine chemical industries.[7] However, preparation of cyclic carbonate by homogeneous catalysis[8] requires high temperature and pressure, besides additional difficulties related to product separation. Alternatively, heterogeneous catalysts for CO_2 fixation, including ionic liquids,[9] silica-supported salts,[10] metal oxides,[11] titanosilicates,[12] organic and metal complexes,[13] organic networks,[14] and microporous polymers[15] mostly demand very high temperatures and/or pressures with multiple purification steps that count for a given chemical process in industry.[16] While traditional catalysts[17] like zeolites,[18] mesoporous silica (MCM-41 and SBA-15), having both acidic and basic pairs, are effective for the cycloaddition reaction, yields from these reactions are often low, and include multiple separation and recycling steps. Therefore, development of efficient catalysts for the synthesis of cyclic carbonates from CO_2 is critical and challenging.[19]

In this regard, CO_2 adsorption with *in situ* conversion, instigating from porous metal-organic frameworks (MOFs), should prove to be a worthy strategy for efficient and profitable reduction of CO_2 emission. Compared to the traditional catalysts (*vide supra*), MOFs show (i) well-defined and tunable pores, (ii) versatile structures, and (iii) possibilities of incorporating acid-base pairs.[20] The definite 3D structure in MOFs offer rational separation between the base functionalities in the organic linkers with adjacent open metal nodes (Lewis acidic) that allow intramolecular reaction between the adsorbed species in these two sites, and prevent catalyst poisoning. Using MOFs, several tetrabutyl ammonium bromide (Bu_4NBr) salt co-catalyzed CO_2 cycloaddition have so far been studied.[21,22] Han *et al.* studied the performance of MOF-5[23] while Ahn *et al.* compared various popular MOFs for the cycloaddition of CO_2 with styrene oxide (SO) in polar

Inorganic Materials & Catalysis Division, CSIR-Central Salt and Marine Chemicals Research Institute, G. B. Marg, Bhavnagar-364 002, Gujarat, India. *E-mail: sneogi@csmcri.res.in*

† *Electronic Supplementary Information (ESI) available: Experimental details, additional figures and tables. See DOI: 10.1039/x0xx00000x*

View Article Online
DOI: 10.1039/C7DT03754F

solvents.[24] However, a serious of drawback in many MOFs that limits their application in catalysis is non availability of active sites, specifically Lewis acidic centres. Though several famous MOFs, including MIL-101, MIL-53, HKUST-1, NU-1000 and UiO-66, have been applied for cycloaddition, these still suffer from lack of functional sites, especially basic sites. Taking advantage of their tunabilities, MOFs can be easily synthesized with Lewis acidic character in the metal nodes, so that they can rapidly activate epoxides. Likewise, incorporation of amine group in MOF has dual advantage as they can act as electron donor (Lewis base) to CO_2 molecule and increase the local concentration of CO_2 near the catalytic centres through high CO_2 adsorption due to the amino effect.[25] In fact, the concerted reaction concepts on acid-base MOFs has been reported by Baiker *et al.* in the synthesis of propylene carbonate with amine-containing mixed-linker.[21a] Based on these rationales, we anticipated that MOF having both, open metal sites and amine functionalization should be suitable for the CO_2 cycloaddition reaction. In this regard, the well-known NH_2-MIL-53(Al)[26] could be a starting point. However, this MOF exhibits a very narrow pore (vnp) configuration after solvent removal, as a result of hydrogen bonding interactions between the -NH_2 group with the aluminium cluster,[27] ultimately leading to poor condensations reactions.[28] In contrast, the kinetically favoured NH_2-MIL-101(Al) framework[29] propagates via sharing the large tetrahedron (also called super tetrahedron, ST), made from trimeric Al^{3+} secondary building units (SBUs), and allows the advantage of generating coordinatively unsaturated metal centres upon desolvation. Moreover, NH_2-MIL-101(Al) is a combination of micro-mesopores that is expected to combine the advantages of each pore size regime,[30] and overcome the limitations of purely microporous or purely mesoporous structures (*vide infra*). To the best of our knowledge, no systematic analysis of the acid-base property in NH_2-MIL-101(Al), specifically cycloaddition reaction of epoxides with CO_2, has yet been reported.

In the light of aforementioned annotations, we synthesized micro-mesoporous NH_2-MIL-101(Al) with well-isolated acid-base pairs and explored its catalytic activity in the solvent-free cycloaddition of CO_2 with styrene oxide in the presence of co-catalyst TBAB to yield styrene carbonates (SC). More than 99% conversion with 96% yield and 99% selectivity with turn over frequency (TOF) of 23.5 h^{-1} was achieved with NH_2-MIL-101(Al)/TBAB system, indicating a synergistic catalysis during CO_2 cycloaddition. The high conversion and selectivity of the catalyst is maintained throughout five cycles, while leaching test does not show any leached Al^{3+} ion. Furthermore, the effects of various reaction parameters like catalyst-cocatalyst ratio, reaction time, temperature and pressure have been investigated in detail for diverse substrates that exhibit outstanding conversions with excellent selectivity is maintained for a range of aliphatic and aromatic epoxide, providing the benefit of micro-mesoporous system.

Experimental section

Materials and methods

All the reagents and solvents were purchased and used without further purification. The powder X-ray diffraction (PXRD) for NH_2-MIL-101(Al) were recorded using X'Pert-MPD Diffractometer with Cu-Kα (λ =1.54056 Å) radiation in the 2θ range 2-50° at a scan speed of 0.1°sec^{-1}. Thermogravimetric analysis (TGA) was studied using 209 F1-Libra (Netzsch, Germany) thermal analyser at a heating rate of 10 °C/minute under N_2 atmosphere. The temperature is ramped from room temperature to 600 °C and percentage mass change (Δm) is plotted as a function of temperature. The FT-IR spectra were recorded using the Perkin Elmer GX-FTIR spectrometer with the wave range of 4000-400 cm^{-1}. The resolution was set to 4 cm^{-1}, and about 200 scans were averaged to one spectrum. The field emission-scanning electron microscopy (FE-SEM) micrographs were recorded on a JSM-7100F scanning electron microscope equipped with energy-dispersive X-ray detector (EDX). The N_2 adsorption isotherm on the desolvated samples were performed using Micromeritics ASAP 2020 analyser, while high pressure gas adsorption was carried out using BELSORP-HP, (BEL Inc. Japan). Prior to adsorption measurements, the as-synthesized frameworks were heated to 120 °C for 5 h under vacuum to produce guest free samples. For dynamic light scattering (DLS) measurements, NaBiTec SpectroSize300 light scattering apparatus (NaBiTec, Germany) with a He−Ne laser (633 nm, 4 mW) was used. The temperature programmed desorption (TPD) were performed using Micromeritics Autochem II. The NMR spectra were recorded using 500 and 600 MHz JEOL NMR spectrometer at ambient temperature in $CDCl_3$ as solvent. The chemical shifts are reported in parts per million (ppm) and the coupling constants *J* are given in hertz (Hz). Data are reported as follows: chemical shift, multiplicity (s-singlet, d-doublet, t-triplet), integration and coupling constant. The residual signal of $CDCl_3$ is δH = 7.26 ppm.

Synthesis of NH_2-MIL-101(Al)

The NH_2-MIL-101(Al) was solvothermally synthesised using the improved method developed by Chmielewski *et al.*[31] based on the earlier report by Gascon *et al.*[32] followed by activation, and was denoted as ***1S***. This synthetic method was also carried out under microwave irradiation as an alternative energy source at 130 °C for 1h at 800W with same starting material to yield similar material, denoted as ***1M***. The detailed experimental procedures are provided in the ESI.**†**

CO_2 fixation with Epoxides

In a typical reaction, 50 mL stainless steel autoclave reactor was equipped with a magnetic stirring bar. The autoclave was first purged with CO_2 (99.99% purity) to remove air and charged with fixed amounts of the catalyst (***1S***, 0.17 mol%), and cocatalyst (TBAB. 0.14 mol%). Next, 105 mmol of SO was charged into the autoclave. The reactor was pressurized with CO_2 up to 18 bar at room temperature, stirred at 800 rpm and maintained the temperature at desired level (120 °C) for 6 h. After completion of reaction, the reactor was allowed to reach room temperature and excess CO_2 was carefully vented off. The above catalytic procedure, with identical quantity of catalyst/co-catalyst and starting materials, was performed under similar reaction condition for the microwave synthesised catalyst ***1M*** as well. The final filtrate was analysed

View Article Online
DOI: 10.1039/C7DT03754F

using NMR spectroscopy to determine the conversion as well as selectivity. The details of NMR spectra of all the synthesised cyclic carbonates are provided in Fig. S11-S23 in ESI.†

Safety Note: The autoclave experiments described in this paper involve the use of high pressure and require equipment with an appropriate pressure rating.

Results and discussion

While MIL-53(Al) framework is thermodynamically favoured product, MIL-101(Al) is kinetically favoured. The crucial observation is the occurrence of an intermediate MOF-235(Al)[29] structure, for which analogous species were earlier recognised during the crystallization of iron carboxylates.[33] Importantly, kinetics can be altered by changing the solvent and metal precursor, resulting in the selective formation of either MIL–53(Al) or MIL-101(Al). Given the presence of -NH_2 functionality in MOF leads to higher CO_2 adsorption and increased hydrolytic stability, as clearly evidenced by the higher stability of IRMOF-3 over IRMOF-1,[34] the amino-substituted NH_2-MIL-101(Al) is prepared (***1S***) by proper tuning of the synthetic conditions.[35] Moreover, NH_2-MIL-101(Al) shows presence of both micro as well as mesopores in a 3D network (Fig. 1 and Fig. S25 in ESI†), which may benefit the free diffusion of substrates, products and solvents in the pores of the framework. In addition, we also synthesized the same MOF (***1M***) by microwave method (ESI†).

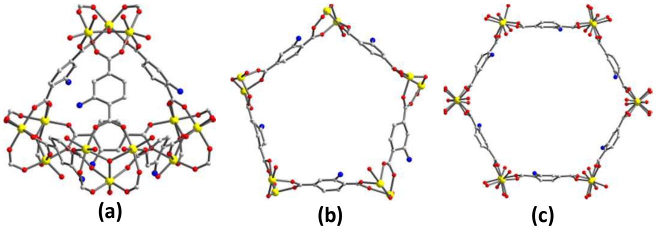

Fig. 1 Visualization of three different cage structures in NH_2–MIL–101(Al), the super tetrahedra (ST) (a) along with pentagonal (b), and hexagonal voids (c).

The phase purity and structural integrity of both solvothermal and microwave synthesized NH_2-MIL-101(Al) were cross-checked by comparing their PXRD patterns with the previous reports[32,36] that clearly verifies the formation of pure phase in both the cases (Fig. S1 and S2 in ESI†). The as-synthesized framework pores are occupied by solvent molecules, which are completely removed under vacuum. Thermogravimetric analysis (TGA) of the individual desolvated framework shows no mass loss till 350 °C (Fig. S3 in ESI†) and the framework is stable up to 400 °C. Moreover, the resemblance in FT-IR spectra for ***1S*** and ***1M*** (Fig. S4 and Fig.S5 in ESI†) to that of reported ones[32] confirms that compositional similarity is preserved in both the cases. Field emission scanning electron microscopy (FE-SEM) was used to study the morphology and particle dimensions of ***1S*** and ***1M***, which revealed (Fig. 2) comparable surface arrangement with rod and plate like morphologies in both the cases.[31] The decomposition of DMF into dimethylammonium ($H_2NMe_2^+$) and carbonate may have played a role in influencing such morphology of the resulting framework.[37] SEM-Energy-dispersive X-ray spectroscopy (EDX) was collected to calculate the ratio of elements present in the framework (Fig.S6 in ESI†).

Alongside, the N_2 adsorption isotherm at 77 K for ***1S*** shows BET surface area of 2074 m^2/g, with the well-known distinctive steps as found for MIL-101 framework (Fig.S7 in ESI†). These two steps are attributed to the filling of two different types of cavities,[38] where the supertetrahedra are filled at low relative pressures ($P/P_0 < 0.05$), while the larger cavities are filled only as pressure increases. It should be noted that microwave synthesized material ***1M*** also exhibits comparable surface area (2025 m^2/g) to that of ***1S***. Obviously, the total pore volume of 550 cm^3 is lower than that of the un-functionalized material because of the free -NH_2 groups residing inside the cavities. Moreover, polar CO_2 molecules (quadrupole moment = 13.4×10^{-40} C m^2; polarizability = 26.3×10^{-25} cm^3) can easily enter into the pores of this framework and shows 21 wt% (106.66 cm^3/g for ***1S***), and 20.16 wt% (102.25 cm^3/g for ***1M***) of CO_2 adsorption up to 15 bar at 298 K (Fig. S8 in ESI†).

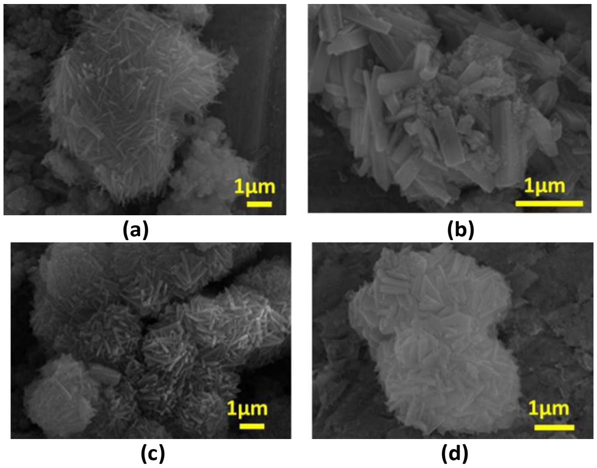

Fig. 2 FE–SEM images of ***1S*** (a, b) and ***1M*** (c, d)

To understand the catalytic activity levels, presence of acidic as well as basic sites were accessed by NH_3 and CO_2 temperature programmed desorption (TPD) profiles (Fig. S9 and Table S1 in ESI†). Finally, the particle size of the framework was measured using dynamic light scattering (DLS) experiment and the hydrodynamic radii (D_h) was found to be 480 nm (Fig. S10 in ESI†).

Catalytic cycloaddition of CO_2 and epoxides

Together, (i) the presence of exposed Al^{3+} metal sites, (ii) pendent amino groups, (iii) high surface area (iv) duel existence of micro and meso-pores, as well as (v) sufficient CO_2 uptake ensures that this framework can be used for CO_2 fixation reaction using epoxides. Prior to the catalytic reaction, the catalyst was activated to remove any physically adsorbed moisture or other guest solvent molecules by vacuum drying at 120 °C for 5 h and finally crushed to fine powder. In the absence of catalyst, the cycloaddition reaction did not afford any product using styrene oxide (SO) as a model substrate, at 18 bar CO_2 pressure and 120 °C even after 12 h (Table 1, entry 1). Alternatively, starting materials (aluminium chloride hexahydrate and 2-amino terephthalic acid) yielded only a trace amount of styrene carbonate (SC) (Table 1, entry 2 and 3). Given that nucleophilic co-catalyst in conjunction with a

View Article Online
DOI: 10.1039/C7DT03754F

Lewis acid is beneficial to produce cyclic carbonates from epoxides and CO_2, tetrabutylammonium bromide (TBAB) was chosen as a suitable candidate. TBAB alone as a catalyst shows only 47% conversion of SO with 99% SC selectivity (Table 1, entry 4). However, TBAB mixed with the aforesaid starting materials produces 48% conversion with 98% selectivity under similar reaction condition (Table 1, entry 5). We speculate that amino group of the ligand may adsorb some CO_2 and further promote the reaction with TBAB. On the other hand, the pristine catalysts, ***1S*** or ***1M*** in the absence of any TBAB, gave 26% and 22% SO conversion, with 78% and 72% selectivity, respectively (Table 1, entry 6 and 7). To our delight, 99% conversion with 96% yield and 99% selectivity is achieved when ***1S***/TBAB system is used under an employed reaction condition of 120 °C, 18 bar CO_2 pressure with 105 mmol of SO, 0.17 mol% of ***1S*** and 0.14 mol% of TBAB in 6 h (Table 1, entry 9). Evidently, the heterogeneous catalyst ***1S***/TBAB offers a multiple fold increase of SC yield compared to any of its precursor materials, indicating the occurrence of a synergistic catalysis during cycloaddition of CO_2 with SO. Under similar reaction condition, the catalytic performance of ***1M*** with TBAB shows almost equal conversion (93.6% SC) with 99% selectivity (Table 1, entry 10). This result highlights the ability of microwave energy not just a rapid route for catalyst synthesis, but also as an efficient means to produce catalysts that maintain the qualities and activities of conventional synthesis. However, room temperature reaction (*vide infra*) yielded only a trace amount of SC (Table 1, entry 8).

Table 1 Cycloaddition of styrene oxide with CO_2 using various starting materials or catalysts

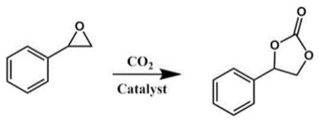

Entry	Catalyst	Temperature (°C)	Conversion (%)	Selectivity (%)	Yield (%)
1	None	120	0	0	0
2	$AlCl_3.6H_2O$	120	Trace	–	–
3	NH_2-BDC	120	Trace	–	–
4	TBAB	120	47	99	–
5	$AlCl_3.6H_2O$ + NH_2-BDC + TBAB	120	48	98	–
6	***1S***	120	26	78	14
7	***1M***	120	22	72	11
8	***1S*** /TBAB	RT	Trace	–	–
9	***1S*** /TBAB	120	99	99	96
10	***1M*** /TBAB	120	93.6	99	95

Effect of reaction parameters

In order to determine the ideal condition for the catalysis, different reaction parameters such as temperature, catalyst amount, CO_2 pressure and reaction time were investigated in detail. At the onset, a series of reactions were conducted with various amount of catalyst loading to find the best SC yield. As depicted in Fig. 3, a gradual increment in the yield was observed from 0.05 to 0.17 mol% of catalyst and no significant changes are observed in the conversion with further catalyst loading (0.2 and 0.25 mol%). Such an observation possibly arises because of the limitation in the mass transfer between the catalyst active sites and reagent, caused by the less dispersion of excess catalyst in the reaction mixture,[39] or due to the achievement of reaction equilibrium.

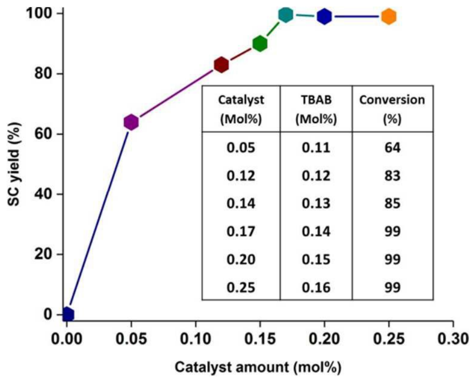

Catalyst (Mol%)	TBAB (Mol%)	Conversion (%)
0.05	0.11	64
0.12	0.12	83
0.14	0.13	85
0.17	0.14	99
0.20	0.15	99
0.25	0.16	99

Fig. 3 Effect of catalyst (***1S***) and TBAB (inset table) in the yield of styrene carbonate (SC). Reaction conditions: SO = 105 mmol, 18 bar CO_2, 6 h, 120 °C. Conversions were determined by ^{1}H NMR spectra (ESI†).

Since a synergism is involved in this catalytic system between the present catalyst/co-catalyst/substrate, the effects of varying the catalyst concentrations with different amount of co-catalyst were also studied. As tabulated in Fig. 3 (Inset), 0.14 mol% of TBAB with 0.17 mol% of ***1S*** was identified as the optimal amount of catalyst that offers maximum SO conversion with 96% SC yield and 99% selectivity. The influence of CO_2 pressure on the conversion of SO was monitored by increasing the pressure, which unveils that the SO conversion is increased with an increase of CO_2 pressure from 2 bar to 22 bar (Fig.4). This could be attributed to an increased solubility of CO_2 at higher pressures and subsequent improvement of CO_2 concentration in the reaction mixture that ultimately shifts the reaction equilibrium to favour the formation of SC. Since ***1S*** exhibits excellent CO_2 adsorption capacity, its highest catalytic activity is observed under 18 bar of CO_2 pressures and it is maintained up to 22 bar.

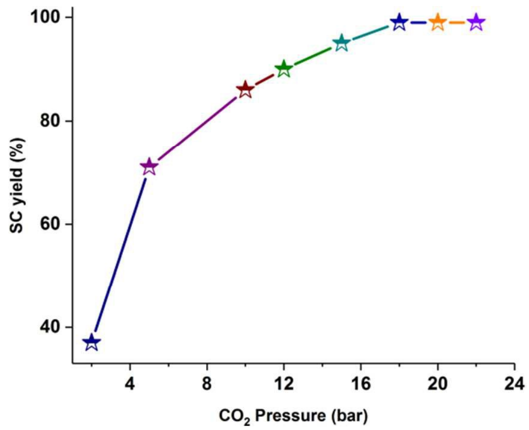

Fig. 4 Effect of CO_2 pressure on the reactivity of SO and CO_2 using 0.17 mol% catalyst at 120 °C in 6h.

View Article Online
DOI: 10.1039/C7DT03754F

Given the lower reaction temperature enhances the possibility of side products formation (diols and dimers),[40] while very high reaction temperature promotes the chances for collapsing of catalyst active sites,[45i] an optimum temperature for catalytic reactions should be evaluated for working multiple times. Therefore, the effect of reaction temperature on the conversion of cyclic carbonates was investigated in the range up to 140 °C (every 20 °C gradients, Fig. 5a), using 18 bar CO_2 pressure, 105 mmol of SO, 0.17 mol% of ***1S*** and 0.14 mol% of TBAB. A multi fold increase in conversion was observed when the temperature gradually ramped from 40 to 120 °C that articulate the effect of heating on cycloaddition reaction.

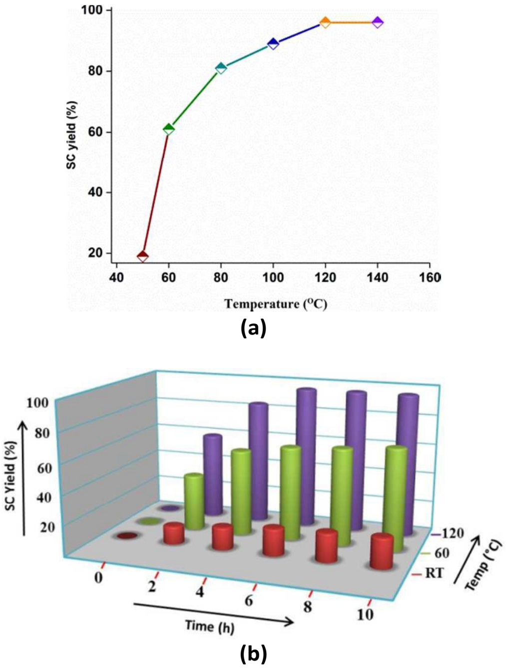

Fig. 5 Formation of SC at different temperature (a), and time variable studies of SC yield at different temperatures (b) using 105 mmol of SO, 18 bar of CO_2 pressure, 0.17 mol% catalyst and 0.14 mol% TBAB.

Below 60 °C the SC yield was low (19%), and above that a sudden increase in SC yield was observed with the maximum of 96% yield at 120 °C. However, the yields remained the same afterwards, inferring that further increase in temperature does not show any major effect on the conversion. The regenerated catalyst maintains its structural integrity, as confirmed from the PXRD pattern (Fig. S2 ESI†).

In order to better understand the catalytic system, we also studied the yield of SC at various temperatures with different time intervals and the results are summarised in Fig. 5b and S24 in ESI†. The product conversion increased with respect to reaction time and the highest conversion was obtained at 6 h. The catalytic reaction performed at room temperature gives only less than 20% of the product and offers 68% yield up to 60 °C. However, the SC yield was maximum at 120 °C up to 6h, and therefore, it was considered the ideal time for reaction. Thus, the optimum conditions for obtaining maximum yields using catalyst ***1S***/TBAB were identified as 6 h duration, 120 °C temperature, and 18 bar of CO_2 pressures contributing to 99% of SO conversion with 99% selectivity. The turnover number (TON) and turnover frequency (TOF) of the catalysts are the standard measures to evaluate the efficiency of a catalyst and it is based on the ratio of mmol of substrate to total active sites with the conversion.

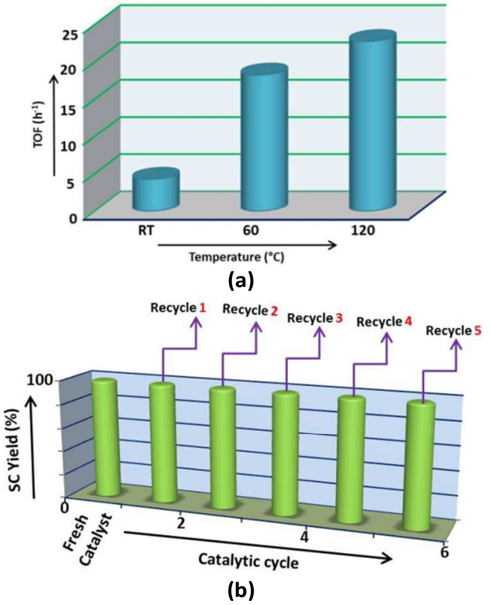

Fig. 6 Turnover frequency (TOF) calculated based on the yield of styrene carbonate at different temperatures (a), recycling ability of the catalyst up to five cycles, showing 99% conversion is maintained throughout under the optimised reaction condition (b).

The TOF for moles of SO converted per mole of active sites of catalyst concentration with 99% conversion was calculated to be 23.5 h^{-1} (TON =141 in 6h) and it is comparable to the previous report.[41] The TOF for other epoxies are listed in Table 3. As shown in Fig. 6a, the TOF experiences almost three fold upsurge, when the temperature is raised from RT to 120 °C. It should be noted that 120 °C is still moderate temperature compared to most of the previous reports[45a] for the synthesis of SC.

Catalyst recycling and leaching test

Another essential factor to be considered in heterogeneous catalysis for both laboratory as well as industrial processes is the catalyst recyclability. For bulk scale production in industrial level, catalyst separation via simple and easier way is economic and environmentally essential to minimize waste streams and develop possible catalyst recycling strategies.[42] To this end, we tested the recyclability of catalyst ***1S*** /TBAB under aforesaid reaction conditions. For this, ***1S*** was recovered by centrifugation after each catalytic cycle, rinsed with chloroform and methanol, and dried in vacuum at 90 °C for the next catalytic run under the similar reaction conditions. To our delight, the high conversion and selectivity is maintained throughout five recycles for the same catalyst (Fig. 6b). The framework ***1S*** preserved its structure throughout the recycling process, as the characteristic peaks remain unchanged in PXRD and FT-IR spectra (Fig. S2 and S5 in ESI†). Alternatively, though hot filtration[43] is considered as a very common method to test the presence of leached metal ions in the reaction medium, the same is not suitable here because of the presence of halide ions in the catalytic system. Therefore, to have an accurate determination of catalyst leaching after reaction, the filtrate

View Article Online
DOI: 10.1039/C7DT03754F

was analysed using inductively coupled plasma optical emission spectrometry (ICP-OES) that shows no trace Al^{3+} ions in the solution even after fifth cycle of the catalyst. The NH_3 and CO_2 TPD profiles were also examined for recycled catalyst, which showed virtually the same profiles as found for the fresh catalyst (Fig. S9 ESI†).

Reaction mechanism and comparison with reported MOFs

In principle, formation of cyclic carbonate is a concerted mechanism, where activation of CO_2 occurs by the nucleophilic attack of a basic group at the carbon atom of CO_2, while the epoxide is activated by adjacent acidic sites. The ring opening is favoured by the co-catalyst, which ultimately reacts with the "activated CO_2" to generate cyclic carbonate. During the catalytic reaction, substrates can diffuse into the pores of the framework that enhances interactions with the reactant molecules. Catalytic activity of NH_2–MIL–101(Al) towards CO_2 fixation with SO suggests that the presence of coordinatively unsaturated Al^{3+} centers in the SBUs act as Lewis acidic sites that coordinate to the epoxides and activate the ring opening, while the amino groups can polarize thermodynamically stable CO_2 molecule and facilitate CO_2 insertion cycloaddition reaction.[44] Based on these rationale, a possible mechanism for the cycloaddition of SO in the presence of ***1S*** and co-catalyst TBAB is illustrated in Scheme 1.

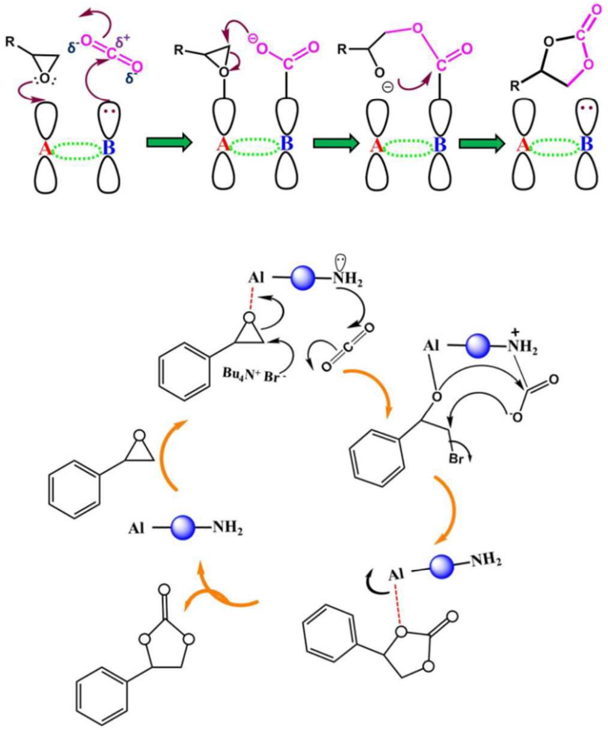

Scheme 1 The general (above) and proposed mechanism (below) for the cycloaddition of SO and CO_2 using ***1S***/TBAB system (A = acidic site; B = basic site).

At the onset, the oxygen atom of SO interacts with the acidic sites (Al^{3+}) of ***1S***, followed by attack of the bulky bromide ions of TBAB to less hindered (β-carbon) carbon atom of epoxide, leading to the opening of the ring. Subsequently, the oxygen atom of the polarized CO_2 molecule attacks the β–carbon of the ring opened epoxide, producing an intermediate with the elimination of bromide ion. Finally, the ring closure takes place to produce SC that subsequently regenerate NH_2-MIL-101(Al), which is further transferred to the next cycle of cycloaddition by coordinating with a new epoxide molecule. Here, it is worthwhile to compare the efficiency of ***1S*** with the earlier reported MOFs towards CO_2–SO fixation reaction. For this, we matched the catalytic abilities of a series of carboxylate based MOFs with that of ***1S*** (Table 2). Though diverse reaction conditions were employed, we attempted a comparison of the MOF catalysts at the closest reaction conditions. The microporous nature of gea-MOF-1, gave 85% conversion of SC up to 20 bar of CO_2 pressure (Table 2, entry 1) and the non-porous nature of $\{Cu(Hip)_2(Bpy)\}_n$ (CHB) (Table 2, entry 3) afford around 70% conversion of SC up to 6 bar pressure of CO_2 at 120 °C in 6h with TBAB as co-catalyst. Under equivalent reaction conditions, ***1S*** with TBAB as co-catalyst gave 99% conversion of SC with 96% yield (Table 2, entry 14). Clearly, ***1S***-TBAB composite system exhibits better catalytic performance compared to several reported MOFs. A notable observation in this study is that the catalytic activity of MOF system, possessing either microporous or non-porous environment, affords less styrene oxide conversion than the MOF with mesoporous system. This observation can be correlated with the easy diffusion of epoxide molecules, having various sizes, (Table 3) inside the mesopores of ***1S***, thereby affording enhanced conversion and selectivity of the primary products such as SC (*vide infra*).

Variation of substrates

The scope and generality of the present catalytic system for CO_2 cycloaddition is further extended with various epoxides (both aliphatic and aromatic) under the aforesaid reaction condition. To our pleasure, high yields were preserved almost in all the cases (Table 3). Nevertheless, aliphatic epoxides gave slight less yields than the aromatic epoxides, which might be attributed to the weaker interactions between the aliphatic chain and the catalyst.[45h] The phenyl glycidyl ether (PGE) gave comparatively outstanding conversions (Table 3, entry 5) with TON as 134 and TOF as 22.3 per mole of catalyst per hour, and the results are essentially better than the reported one[45c,i] under similar condition. Apart from that, aromatic epoxides consume more time to pass through the pores of the framework than the aliphatic epoxides. Therefore, a better mass transfer between catalytic sites and the CO_2 molecule is anticipated. Such good catalytic performance is attributed to the combined effects of available acidic and basic sites, as well as presence of the micro-mesoporosity in ***1S***. However, cyclohexene oxide inhibits the formation of corresponding cyclic carbonate (Table 3, entry 6) and shows reasonably low conversion (15%). This anomaly can be ascribed to the hindrance in anionic attack posed by the steric crowding of the cyclohexene ring. Overall, the present micro-mesoporous material with high surface area and proper functionalization[46] offers excellent catalytic CO_2 fixation reaction under controlled experimental condition, leading to significant yield in the presence of the co-catalyst TBAB.

View Article Online
DOI: 10.1039/C7DT03754F

Table 2 Comparison of the catalytic activities of the NH_2-MIL-101(Al) catalyst with previously reported MOF catalysts along with the employed reaction conditions.

Entry	Catalyst [a]	Structure	Pressure (bar)	Temperature (°C)	Time (h)	Conversion (%)	Yield (%)	Ref [45]
1	gea–MOF–1	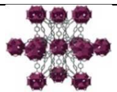	20	120	6	85.0	–	a
2	UMCM–1–NH_2	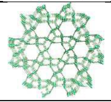	12	RT	24	53.0	53	b
3	{Cu(Hip)$_2$(Bpy)}n (CHB)	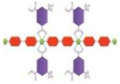	12	120	6	69.8	56	c
4	$[Cu_2L(H_2O)_2]\cdot4H_2O\cdot2DMF$	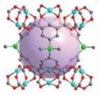	10	100	6	64.1	–	d
5	MIL–68(In) –NH_2	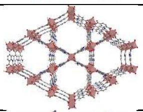	8	150	8	74.0	–	e
6	MOF–5	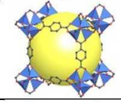	1	50	15	–	92	f
7	MIL–101(Cr)	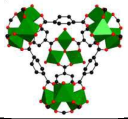	8	25	48	98.0	–	g
8	UiO–67–IL	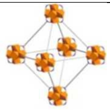	1	90	12	–	98	h
9	ZIF–67	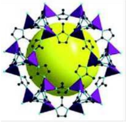	10	100	15	92.0	–	i
10	MOF–205(M)	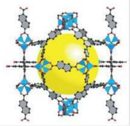	12	RT	24	58.0	58	j
11	3D–CCB	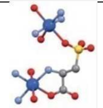	1	100	12	65.9	–	k
12	ZIF–8 [b]	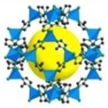	7	100	10	–	55	l
13	HKUST–1	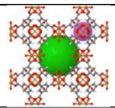	20	100	4	48.0	–	m
14	NH_2–MIL–101(Al)	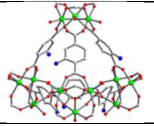	18	120	6	99.0	96	*

[a]with co–catalyst = Tetrabutyl ammonium bromide (TBAB), [b]without co-catalyst, *present work.

View Article Online
DOI: 10.1039/C7DT03754F

Table 3 Cycloaddition of CO_2 with various epoxide substrates using the NH_2-MIL-101(Al)/TBAB catalyst.[a]

Entry	Product	Conversion[b] (%)	Selectivity (%)	Yield[c] (%)	TON	TOF[d] (h^{-1})
1	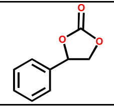	99	>99	96	141	23.5
2	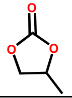	96	99	95	130	21.7
3	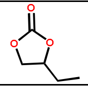	98	99	96	133	22.2
4	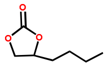	94	99	94	127	21.2
5	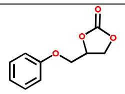	99	99	97	134	22.3
6	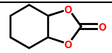	15	99	15	20	3.3

[a]Reaction conditions: 120 °C, 18 bar CO_2 pressure, solvent- free, epoxides –105 mmol, ***1S***–0.17 mol%, TBAB–0.14 mol%. [b]Based on ^1H NMR spectrum of reaction mixture aliquots without further purification. [c] Based on isolated product. [d]TOF (turnover frequency): Moles of product formed per mole of catalyst per hour.

Conclusion

In conclusion, the highly stable framework NH_2-MIL-101(Al) has been successfully synthesised by both solvothermal (***1S***) as well as microwave energy (***1M***) and characterised through PXRD, FT-IR, TGA, SEM-EDX and BET surface area analysis. Presence of suitable acid/base pairs and the micro-mesoporosity of the framework, together with excellent high pressure CO_2 adsorption provide a platform to utilize the MOF in the chemical fixation of CO_2 by cycloaddition reactions with various epoxides. The solvent free cycloaddition reactions for ***1S*** in the presence co-catalyst TBAB, using CO_2 and styrene oxide demonstrates a synergistic catalysis of ***1S***/TBAB system that resulted more than 99% conversion with 96% yield and 99% selectivity, having turn over frequency (TOF) of 23.5 h^{-1}. Likewise, ***1M*** gives 93.6% conversion with 95% yield and 99% selectivity. Thorough analysis of various reaction parameters revealed that optimum conditions for obtaining maximal yield with highest selectivity for the cyclic carbonate are 6 h duration, 120 °C temperature, and 18 bar of CO_2 pressures. The recyclability test of catalyst showed high conversion and selectivity is maintained throughout five cycles, while leaching test does not show even a trace amount of leached Al^{3+} ion, signifying that the present catalytic system is suitable in extending its scope from academia and research, to industrial perspectives. Moreover, outstanding conversion and selectivity is maintained for both aliphatic and aromatic epoxides under the similar reaction condition. This in turn supplement that present micro-mesoporous hybrid material is more efficient towards CO_2 cycloaddition, with smaller as well as bulkier epoxides, compared to many reported MOFs. Overall, the hybrid nature of NH_2-MIL-101(Al), having pendent amino group, offers easy accessibility to a range of reactant molecules inside its pores and represents a valuable family member for MOFs to future heterogeneous catalysis in CO_2 cycloaddition reaction.

Acknowledgements

S. N. acknowledges the financial support from DST-SERB (Grant No. ECR/2016/000156), S. S. acknowledges CSIR Network project (Grant No. CSC-0122). The analytical support from ADCIF is greatly acknowledged. CSMCRI Communication No. 141/2017

Notes and references

1 (a) S. Solomon, G.-K. Plattner, R. Knutti and P. Friedlingstein, *Proc. Natl. Acad. Sci. U.S.A*, 2009, **106**, 1704–1709; (b) J. Hansen, M. Sato, R. Ruedy, K. Lo, D. W. Lea and M. M. Elizade, *Proc. Natl. Acad. Sci. U. S. A*, 2006, **103**, 14288–14293.
2 (a) A. A. G. Shaikh and S. Sivaram, *Chem. Rev*, 1996, **96**, 951–976; (b) T. Sakakura and K. Kohno, *Chem. Commun*, 2009, 1312–1330.
3 (a) M. Cokoja, C. Bruckmeier, B. Rieger, W. A. Herrmann and F. E. Kühn, *Angew. Chem. Int. Ed*, 2011, **50**, 8510–8537; (b) I. Omae, *Coord. Chem. Rev*, 2012, **256**, 1384–1405.
4 (a) J. Roeser, K. Kailasam and A. Thomas, *ChemSusChem*, 2012, **5**, 1793–1799; (b) T. Lescouet, C. Chizallet and D. Farrusseng, *ChemCatChem*, 2012, **4**, 1725–1728.
5 H. L. Parker, J. Sherwood, A. J. Hunt and J. H. Clark, *ACS Sustainable Chem. Eng*, 2014, **2**, 1739–1742.
6 (a) M. Petrowsky, M. Ismail, D. T. Glatzhofer and R. Frech, *J. Phys. Chem. B*, 2013, **117**, 5963–5970; (b) G. -C. Chung, H. -J. Kim, S. -H. Jun and M. -H. Kim, *Electro chem*, 1999, **1**, 493–496.
7 (a) K. Biggadike, R. M. Angell, C. M. Burgess, R. M. Farrell, A. P. Hancock, A. J. Harker, A. J. Irving, W. R. Irving, C. Ioannou, P. A. Procopiou, R. E. Shaw, Y. E. Solanke, O. M. P. Singh, M. A. Snowden, R. Stubbs, S. Walton and H. E. Weston, *J. Med. Chem*, 2000, **43**, 19–21; (b) A. -A. G. Shaikh and S. Sivaram, *Chem. Rev*, 1996, **96**, 951–976.
8 (a) N. Kihara, N. Hara and T. Endo, *J. Org. Chem*, 1993, **58**, 6198–6202; (b) H. Yasuda, L. N. He, T. Sakakura and C. Hu, *J. Catal*, 2005, **233**, 119–122.

View Article Online
DOI: 10.1039/C7DT03754F

9 (a) J. Sun, S. I. Fujita and M. Arai, *J. Organometal. Chem*, 2005, **690**, 3490–3497; (b) Q. He, J. W. O'Brien, K. A. Kitselman, L. E. Tompkins, G. C. T. Curtisa and F. M. Kerton, *Catal. Sci. Technol*, 2014, **4**, 1513–1528.

10 J. Q. Wang, D. L. Kong, J. Y. Chen, F. Cai and L. N. He, *J. Mol. Catal. A Chem*, 2006, **249**, 143–148.

11 (a) T. Yano, H. Matsui, T. Koike, H. Ishiguro, H. Fujihara and M. Yoshihara, *Chem. Commun*, 1997, 1129–1130; (b) K. Yamaguchi, K. Ebitani, T. Yoshida, H. Yoshida and K. Kaneda, *J. Am. Chem. Soc*, 1999, **121**, 4526–4527; (c) H. Yasuda, L.N. He, T. Sakakura, *J. Catal*, 2002, **209**, 547–550; (d) H. Yasuda, L.N. He, T. Sakakura and C.W. Hu, *J. Catal*, 2005, **233**, 119–122.

12 R. Srivastava, D. Srinivas and P. Ratnasamy, *J. Catal*, 2005, **233**, 1–15.

13 (a) R. L. Paddock and S. T. Nguyen, *J. Am. Chem. Soc*, 2001, **123**, 11498–11499; (b) J. Wang, J. Wu and N. Tang, *Inorg. Chem. Commun*, 2007, **10**, 1493–1495.

14 J. Chun, S. Kang, N. Kang, S. M. Lee, H. J. Kim and S. U. Son, *J. Mater. Chem. A*, 2013, 5517–5523.

15 Y. Xie, T. T. Wang, X. H. Liu, K. Zou and W. Q. Deng, *Nat. Commun*, 2013, **4**, 1960–1966.

16 D. J. Darensbourg and M. W. Holtcamp, *Chem. Rev*, 1996, **96**, 155–174; (b) M. M. Dharman, J. I. Yu, J. Y. Ahn and D. W. Park, *Green Chem*, 2009, **11**, 1754–1757.

17 (a) M. Tu and R. J. Davis, *J. Catal*, 2001, **199**, 85–91; (b) Y. Li, X. -Q. Zhao, Y. -J. Wang, *Appl. Catal A: G*, 2005, **279**, 205–208; (c) R. Srivastava, D. Srinivas and P. Ratnasamy, *Microporous Mesoporous Mater*, 2006, **90**, 314–326.

18 E. J. Doskocil, S. V. Bordawekar, B. G. Kaye and R. J. Davis, *J. Phys. Chem. B*, 1999, **103**, 6277–6282.

19 D. W. Kim, R. Roshan, J. Tharun, A. C. Kathalikkattil and D. W. Park, *Korean J. Chem. Eng*, 2013, **30**, 1973–1984.

20 (a) J. Kim, S. N. Kim, H. G. Jang, G. Seo and W. S. Ahn, *Appl. Catal. A Gen*, 2013, **453**, 175–180; (b) S. M. J. Rogge, A. Bavykina, J. Hajek, H. Garcia, A. I. Olivos-Suarez, A. Sepu´lveda-Escribano, A. Vimont, G. Clet, P. Bazin, F. Kapteijn, M. Daturi, E. V. Ramos-Fernandez, F. X. Llabre´s i Xamena, V. Van Speybroeck, J. Gascon, *Chem. Soc. Rev*, 2017, **46**, 3134–3184.

21 (a) W. Kleist, F. Jutz, M. Maciejewski and A. Baiker, *Eur. J. Inorg. Chem*, 2009, 3552–3561; (b) X. Zhou, Y. Zhang, X. G. Yang, L. Z. Zhao and G. Y. Wang, *J. Mol. Catal. A Chem*, 2012, **361**, 12–16; (c) J. Kim, S. N. Kim, H. G. Jang, G. Seo and W. S. Ahn, *Appl. Catal. A Gen*, 2013, **453**, 175–180; (d) Y. J. Kim and D.W. Park, *J. Nanosci. Nanotechnol*, 2013, **13**, 2307–2312.

22 (a) D. A. Yang, H. Y. Cho, J. Kim, S.T. Yang and W. S. Ahn, *Energy Environ. Sci*, 2012, **5**, 6465–6473; (b) T. Lescouet, C. Chizallet, and D. Farrusseng, *ChemCatChem*, 2012, **2**, 1725–1728; (c) O. Zalomaeva, A. M. Chibiryaev, K. A. Kovalenko, O. A. Kholdeeva, B. S. Balzhinimaev and V. P. Fedin, *J. Catal*, 2013, **298**, 179–185; (d) A. C. Kathalikkattil, R. Roshan, J. Tharun, H. G. Seok, H. S. Ryu and D. W. Park, *ChemCatChem*, 2014, **6**, 284–292; (e) D. De, T. K. Pal, S. Neogi, S. Senthilkumar, D. Das, S. S. Gupta and P. K. Bharadwaj, *Chem. Eur. J*, 2016, **22**, 3387–3396.

23 J. Song, Z. Zhang, S. Hu, T. Wu, T. Jiang and B. Han, *Green. Chem*, 2009, **11**, 1031–1036.

24 J. Kim, S. N. Kim, H. G. Jang, G. Seo and W. S. Ahn, *Appl. Catal. A Gen*, 2013, **453**, 175–180.

25 (a) A. Torrisi, R. G. Bell and C. M. -Draznieks, *Cryst. Growth Des*, 2010, **10**, 2839–2841; (b) E. Stavitski, E. A. Pidko, S. Couck, T. Remy, E. J. M. Hensen, B. M. Weckhuysen, J. Denayer, J. Gascon and F. Kapteijn, *Langmuir*, 2011, **27**, 3970–3976; (c) J. G. Vitillo, M. Savonnet, G. Ricchiardi and S. Bordiga, *ChemSusChem*, 2011, **4**, 1281–1290.

26 B. Arstad, H. Fjellvag, K. O. Kongshaug, O. Swang and R. Blom, *Adsorption*, 2008, **14**, 755-762.

27 (a) E. Stavitski, E. Pidko, S. Couck, T. Remy, E. Hensen, B. Weckhuysen, J. F. M. Denayer, J. Gascon, F. Kapteijn, *Langmuir*, 2011, **27**, 3970-3976; (b) S. Couck, E. Gobechiya, C. E. A. Kirschhock, P. Serra-Crespo, J. Juan-Alcañiz, A. Martinez-Joaristi, E. Stavitski, J. Gascon, F. Kapteijn, G. V. Baron, J. F. M. Denayer, *ChemSusChem*, 2012, **5**, 740-750; (c) P. Serra-Crespo, M. A. van der Veen, E. Gobechiya, K. Houthoofd, Y. Filinchuk, C. E. A. Kirschhock, J. A. Martens, B. F. Sels, D. E. De Vos, F. Kapteijn and J. Gascon, *J. Am. Chem. Soc*, 2012, **134**, 8314–8317.

28 Y. Lin, C. Kong and L. Chen, *RSC Adv*, 2016, **6**, 32598–32614.

29 E. Stavitski, M. Goesten, J. Juan-Alcaniz, A. Martinez-Joaristi, P. Serra-Crespo, A.V. Petukhov, J. Gascon, F. Kapteijn, *Angew. Chem. Int. Ed*, 2011, **50**, 9624–9628.

30 (a) M. H. Beyzavi, R. C. Klet, S. Tussupbayev, J. Borycz, N. A. Vermeulen, C. J. Cramer, J. F. Stoddart, J. T. Hupp and O. K. Farha, *J. Am. Chem. Soc*, 2014, **136**, 15861–15864; (b) M. H. F. Kox, E. Stavitski, J. C. Groen, J. Pérez-Ramírez, F. Kapteijn and B. M. Weckhuysen, *Chem. Eur. J*, 2008, **14**, 1718-1725; (c) J. Roeser, K. Kailasam and A. Thomas, *ChemSusChem*, 2012, **5**, 1793–1799; (d) M. Zhu and M. A. Carreon, *J. Appl. Polym. Sci*, 2014, **131**, 39738–39750.

31 A. Choluj, A. Zieliński, K. Grela and M. J. Chmielewski, *ACS Catal*, 2016, **6**, 6343–6349.

32 P. S. Crespo, E. V. R. Fernandez, J. Gascon and F. Kapteijn, *Chem. Mater*, 2011, **23**, 2565–2572.

33 (a) A. C. Sudik, A. P. Cote and O. M. Yaghi, *Inorg. Chem*, 2005, **44**, 2998–3000; (b) F. Millange, M. I. Medina, N. Guillou, G. Ferey, K. M. Golden and R. I. Walton, *Angew. Chem. Int. Ed*, 2010, **49**, 763–766.

34 (a) X. Zhang, F. X. Llabrés i Xamena and A. Corma, *J. Catal*, 2009, **265**, 155–160; (b) M. J. Ingleson, J. P. Barrio, J.-B. Guilbaud, Y. Z. Khimyak and M. J. Rosseinsky, *Chem. Commun*, 2008, 2680–2682; (c) Z. Q. Wang and S. M. Cohen, *Chem. Soc. Rev*, 2009, **38**, 1315–1329.

35 (a) T. Ahnfeldt, D. Gunzelmann, T. Loiseau, D. Hirsemann, J. Senker, G. Ferey and N. Stock, *Inorg. Chem*, 2009, **48**, 3057–3064; (b) M. G. Goesten, P. C. M. M. Magusin, E. A. Pidko, B. Mezari, E. J. M. Hensen, F. Kapteijn and J. Gascon, *Inorg. Chem*, 2014, **53**, 882–887.

36 (a) L. Qin, Z. Li, Q. Hu, Z. Xu, X. Guo and G. Zhang, *Chem. Commun*, 2016, **52**, 7110–7113; (b) L. Bromberg, X. Su and T. A. Hatton, *ACS Appl. Mater. Interfaces*, 2013, **5**, 5468–5477.

37 (a) J. An, O. K. Farha, J. T. Hupp, E. Pohl, J. I. Yeh and N. L. Rosi, *Nat. Commun*, 2012, **3**, 604–609; (b) L. Wang, W. Yang, Y. Li, Z. Xie, W. Zhua and Z. M. Sun, *Chem. Commun*, 2014, **50**, 11653—11656.

38 D.-Y. Hong, Y. K. Hwang, C. Serre, G. Ferey and J.-S. Chang, *Adv. Funct. Mater*, 2009, **19**, 1537–1552.

39 A. C. Kathalikkattil, J. Tharun, R. Roshan, H. G. Soek and D. W. Park, *Appl. Cata. A*, 2012, **107**, 447–448.

40 (a) E. E. Macias, P. Ratnasamy and M. A. Carreon, *Catal Today*, 2012, **198**, 215–218; (b) A. C. Kathalikkattil, R. Babu, J. Tharun, R. Roshan and D. W. Park, *Catal. Surv. Asia*, 2015, **19**, 223–235.

41 A. C. Kathalikkattil, R. Babu, R. Roshan, H. Lee, H. Kim, J. Tharun, E. Suresh and D. W. Park, *J. Mater. Chem. A*, 2015, **3**, 22636–22647.

42 M. Arai and F. Zhao, *Catalysts*, 2015, **5**, 868–871.

43 R. A. Sheldon, M. Wallau, I. W. C. E. Arends and U. Schuchardt, *Acc. Chem. Res*, 1998, **31**, 485–493.

44 M. Zhu and M. A. Carreon, *J. Appl. Polym. Sci*, 2014, **131**, 39738–39750.

45 a) V. Guillerm, L. J. Weseliński, Y. Belmabkhout, A. J. Cairns, V. D'Elia, L. Wojtas, K. Adil and M. Eddaoudi, *Nat. Chem*, 2014, **6**, 673–680; b) R. Babu, A. C. Kathalikkattil, R. Roshan, J. Tharun, D. W. Kim and D. -W. Park, *Green Chem*, 2016, **18**, 232–242; c) A. C. Kathalikkattil, D. W. Kim, J. Tharun, H. -G.

View Article Online
DOI: 10.1039/C7DT03754F

Soek, R. Roshan and D. W. Park, *Green Chem*, 2014, **16**, 1607–1616; d) C. -Y. Gao, H. -R. Tian, J. Ai, L. -J. Li, S. Dang, Y. -Q. Land and Z. -M. Sun, *Chem. Commun*, 2016, **52**, 11147–11150; e) T. Lescouet, C. Chizallet and D. Farrusseng, *ChemCatChem*, 2012, **4**, 1725–1728; f) J. Song, Z. Zhang, S. Hu, T. Wu, T. Jiang and B. Han, *Green. Chem*, 2009, **11**, 1031–1036; g) O. V. Zalomaeva, A. M. Chibiryaev, K. A. Kovalenko, O. A. Kholdeeva , B. S. Balzhinimaev , V. P. Fedin, *J. Catal*, 2013, **298**, 179–185; h) L. -G Ding, B. -J. Yao, W. -L. Jiang, J. -T. Li, Q. -J. Fu, Y. -A. Li, Z. -H. Liu, J. -P. Ma and Y. -B. Dong, *Inorg. Chem*, 2017, **56**, 2337–2344; i) B. Mousavi, S. Chaemchuen, B. Moosavi, Z. Luo, N. Gholampour and F. Verpoort, *New J. Chem*, 2016, **40**, 5170–5176; j) R. Babu, R. Roshan, A. C. Kathalikkattil, D. W. Kim and D. W. Park, *ACS Appl. Mater. Interfaces*, 2016, **8**, 33723−33731; k) A. C. Kathalikkattil, R. Roshan, J. Tharun, H. -G. Soek, H. -S. Ryu and D. W. Park, *ChemCatChem*, 2014, **6**, 284–292; l) M. Zhu, D. Srinivas, S. Bhogeswararao, P. Ratnasamy and M. A. Carreon, *Catal Commun*, 2013, **32**, 36–40; m) J. Kim, S. N. Kim, H. G. Jang, G. Seo and W. S. Ahn, *Appl. Catal. A Gen*, 2013, **453**, 175–180.

46 J. Wang, W. Sng, G. Yi and Y. Zhang, *Chem. Commun*, 2015, **51**, 12076–12079.

View Article Online
DOI: 10.1039/C7DT03754F

Table of Content

NH_2–MIL–101(Al)/*n*–Bu_4NBr works as excellent solvent free catalyst for CO_2 cycloaddition with epoxides, and highlights the benefits of micro-mesoporous system with acidic and basic functionalities.